

¹ Timescales for the Penetration of IMF B_y into the ² Earth's Magnetotail

S. D. Browett¹, R. C. Fear¹, A. Grocott², S. E. Milan^{3, 4}

Corresponding author: S. D. Browett, Department of Physics and Astronomy, University of Southampton, Southampton, Hampshire, SO17 1BJ, United Kingdom. (s.browett@soton.ac.uk)

¹Department of Physics and Astronomy,
University of Southampton, Southampton,
Hampshire, SO17 1BJ, UK

²Department of Physics, Lancaster
University, Lancaster, UK

³Department of Physics and Astronomy,
University of Leicester, Leicester, UK

⁴Birkeland Centre for Space Sciences,
University of Bergen, Norway

Key Points.

- Dayside reconnection can introduce a B_y component into the magnetosphere, in the same sense as the IMF B_y .
- The Dungey cycle transfers field lines with this induced B_y component into the magnetotail.
- The timescale for this process is found to be between 1-5 hours, depending on a few contributing factors.

Abstract.

Previous studies have shown there is a correlation between the B_y component of the interplanetary magnetic field (IMF) and the B_y component observed in the magnetotail lobe and in the plasma sheet. However, studies of the effect of IMF B_y on several magnetospheric processes have indicated that the B_y component in the tail should depend more strongly on the recent history of the IMF B_y rather than on the simultaneous measurements of the IMF. Estimates of this timescale vary from ~ 15 minutes to ~ 4 hours. We present a statistical study of how promptly the IMF B_y component is transferred into the neutral sheet, based on Cluster observations of the neutral sheet from 2001 to 2008, and solar wind data from the OMNI database. 5982 neutral sheet crossings during this interval were identified, and starting with the correlation between instantaneous measurements of the IMF and the magnetotail (recently reported by *Cao et al.* [2014]), we vary the time delay applied to the solar wind data. Our results suggest a bimodal distribution with peaks at ~ 1.5 and ~ 3 hours. The relative strength of each peak appears to be well controlled by: the sign of the IMF B_z component with peaks being

20 observed at 1 hour of lag time for southward IMF and up to 5 hours for north-
21 ward IMF conditions, and the magnitude of the solar wind velocity with peaks
22 at 2 hours of lag time for fast solar wind and 4 hours for slow solar wind con-
23 ditions.

1. Introduction

24 The main interaction between the solar wind and the magnetosphere is through the
25 process of magnetic reconnection. Reconnection occurs most favourably when two oppo-
26 sitely directed fields in two plasmas encounter each other; this is the case at Earth when
27 the north-south component of the Interplanetary Magnetic Field (IMF B_z) is negative.
28 Reconnection between the IMF and terrestrial magnetic field drives the dynamics of the
29 magnetosphere through a mechanism called the Dungey cycle [Dungey, 1961], leading to
30 the open magnetosphere model.

31
32 *Fairfield* [1979] showed that there is a positive correlation between the B_y component in
33 the magnetotail and the IMF B_y component. B_y data taken from the IMP 6 satellite of the
34 entire breadth of the magnetotail, at $20R_e$ - $33R_e$ down the magnetotail, from 1971 to 1974
35 were plotted against hourly averages of measurements of IMF B_y . Fairfield calculated the
36 gradient of the best fit line (the penetration efficiency) and found a weak penetration of
37 0.13; they did not report a value for the correlation coefficient, but the significant scatter
38 in their Figure 9 indicates that the correlation must be low. *Cowley* [1981a] explained this
39 observation as a consequence of the open magnetosphere model. Newly opened field lines
40 on the day side have a B_y component, which is transferred into the magnetotail lobes as
41 the field lines convect into the lobes. The B_y asymmetry is then transferred onto closed
42 field lines when the asymmetric lobe field lines undergo magnetotail reconnection. The
43 word “penetration”, in terms of the IMF exerting an influence on magnetospheric field
44 lines, can be misleading. The IMF does not enter the magnetosphere, instead the field

45 lines associated with the IMF connect to magnetospheric field lines which then allows the
46 IMF to act upon the magnetosphere, inducing a B_y component in the magnetosphere in
47 the same sense as in the IMF. The choice to use the word “penetration” is for consistency
48 in terminology with previous studies.

49
50 Since *Fairfield* [1979] there have been further studies showing the correlation between
51 instantaneous measurement of the IMF B_y and the magnetotail B_y [*Tsurutani et al.*, 1984;
52 *Hilmer and Voigt*, 1987; *Nagai*, 1987; *Sergeev*, 1987; *Voigt and Hilmer*, 1987; *Hau and*
53 *Erickson*, 1995; *Newell et al.*, 1995; *Wing et al.*, 1995; *Petrukovich*, 2009] which have
54 reported penetration efficiencies ranging from 0.1-0.6; a review by *Kaymaz et al.* [1994] is
55 also available. *Nishida et al.* [1995] has reported a penetration efficiency of 0.25 in the dis-
56 tant tail during instances of lobe reconnection (northward IMF) with a dominant IMF B_y
57 component. A mechanism for IMF penetration under northward IMF conditions, which
58 explains the observations made by *Nishida et al.* [1995], has been proposed in *Nishida*
59 *et al.* [1998] and simulated in *Nishida and Ogino* [1998]. Other studies have investigated
60 how IMF B_y affects the polar cap convection cell pattern [*Moses et al.*, 1985].

61
62 *Petrukovich* [2011] discussed the sources of B_y components in the magnetotail; they
63 found that the largest source of B_y in the magnetotail is from IMF B_y penetration, and
64 listed the following (more minor) effects:

65 1. Magnetotail flaring is the effect where magnetospheric magnetic field lines are con-
66 nected to the ionosphere, and therefore away from the the magnetotail axis they have a
67 B_y component. *Petrukovich* estimates that at $Y_{GSM}=\pm 10R_e$ there will be an addition of

68 plasma sheet B_y that is approximately equal to 40% of the plasma sheet B_x component.
69 This effect is equal and opposite in the northern and southern hemispheres and so it can-
70 cels out at the neutral sheet (the interface between the inward and outward pointing field
71 lines of the northern and southern hemispheres respectively).

72 2. Neutral sheet warping is the situation where the flanks of the neutral sheet warp
73 southward and the centre of the neutral sheet deflects northwards in the summer, and
74 oppositely for the winter. This effect is relatively small, having been estimated by
75 *Petrukovich* [2011] to contribute approximately ± 1.75 nT to the B_y component in the
76 plasma sheet.

77 3. Another addition of B_y into the magnetotail is due to the even tilt effect, where the
78 neutral sheet twists to remain normal to the line connecting each end of the dipole. This
79 means that the even tilt effect is positively correlated with the orientation of the dipole
80 tilt. It has been estimated [*Petrukovich*, 2011] that this effect contributes up to 2nT to
81 the B_y component of the plasma sheet.

82 4. Magnetotail twisting occurs when IMF field lines with a B_y component open the
83 Earth's magnetic field lines (through reconnection) and exert a torque which acts to
84 straighten the open field lines by twisting the magnetotail. *Petrukovich* [2011] estimates
85 that this effect induces an additional B_y component to the plasma sheet that is approxi-
86 mately equal to 10% of the IMF B_y component. *Petrukovich* [2011] states however that
87 this source of B_y in the magnetotail can be considered as a part of IMF penetration as it
88 also is solely dependent on IMF B_y .

89

90 To measure these effects, *Petrukovich* performed his analysis in geocentric solar wind
91 (GSW) coordinates in which the x-axis is anti-parallel to the solar wind flow direction
92 and the x-z plane is defined to contain the dipole axis so that only external effects on the
93 magnetotail are measured. *Petrukovich* also found that the difference between GSW and
94 GSM coordinates (whose x-z plane also contains the dipole axis but the x-axis is directed
95 towards the Sun) is marginal and so performing the analysis in GSM coordinates does
96 not offer any disadvantage in the accuracy of the analysis.

97
98 The correlation of magnetotail B_y with IMF B_y was further examined by *Cao et al.*
99 [2014]. *Cao et al.* specifically restricted their study to the B_y component observed at
100 the neutral sheet, and used several criteria to look exclusively at the neutral sheet during
101 geomagnetically quiet conditions. By studying the B_y component at the neutral sheet
102 *Cao et al.* excluded B_y contribution from magnetotail flaring as the flaring components
103 either side of the neutral sheet are equal and opposite. By using data taken at the neutral
104 sheet and ignoring the relatively small B_y components induced by neutral sheet warp-
105 ing, magnetotail twisting and the even tilt effect, the contribution from only magnetotail
106 penetration is measured. *Cao et al.* defined ‘quiet conditions’ as when there were (i) no
107 changes in solar wind dynamic pressure (either in relative or absolute terms) within 5
108 minutes of a neutral sheet crossing, (ii) no changes in the sign of the IMF B_z component
109 within 5 minutes of a neutral sheet crossing and (iii) no fast flows in the neutral sheet at
110 the time of a neutral sheet crossing. *Cao et al.* found that by restricting their study to the
111 neutral sheet, and by implementing these criteria, a much higher penetration efficiency

112 was found: 0.72 compared to 0.13 in *Fairfield* [1979].

113

114 Most of the above studies have investigated the link between B_y values observed in
115 the magnetotail and the instantaneous IMF B_y component (averaging up to a 1 hour lag
116 time). However, it has been estimated that the Dungey cycle of reconnection should take
117 on the order of a few hours for a field line to convect from the dayside into the magnetotail
118 [*Dungey*, 1965; *Cowley*, 1981b; *Fear and Milan*, 2012a], though this estimate has been
119 rarely tested directly. One way in which the timescales associated with the Dungey cycle
120 have been indirectly investigated is through the study of transpolar arcs. Transpolar arcs
121 are sun-aligned large scale auroral features which form in the polar cap during periods
122 of northward IMF [*Frank et al.*, 1982]. It has been argued that they are formed by the
123 process of magnetotail reconnection during periods of northward IMF, and hence that the
124 local time at which a transpolar arc forms should depend on the B_y component at the
125 neutral sheet which in turn should depend on the recent history of the IMF B_y compo-
126 nent [*Milan et al.*, 2005]. *Fear and Milan* [2012a, b] carried out a statistical study into
127 the formation of 131 transpolar arcs, and showed that the magnetic local times at which
128 transpolar arcs formed was more strongly dependent on the IMF 3-4 hours before the arc
129 formed, which was argued to be indicative of the timescales taken for field lines to convect
130 from the dayside magnetopause to the neutral sheet. However, although the observed
131 correlation between the magnetic local time at which the transpolar arcs formed and the
132 IMF B_y component peaked when the IMF was lagged by 3-4 hours, the correlation was
133 elevated compared with its zero-lag value over a wide range of lag times, from 1 to 10
134 hours. *Grocott and Milan* [2014] have incorporated timescales into a study on the mor-

135 phology of ionospheric convection patterns. They produced average convection patterns
136 for different IMF clock angles, where those clock angles were also binned according to how
137 long the IMF had remained in that orientation. They observed that the convection cell
138 patterns begin to respond within 30 minutes of constant IMF conditions with the convec-
139 tion cell patterns continuing to evolve on the order of hours of constant IMF clock angle.
140 A timescale of hours is in agreement with arguments put forward by *Dungey* [1965], *Cow-*
141 *ley* [1981b] and *Fear and Milan* [2012a] who argue that the convection of magnetic field
142 lines from the day side to the night side should take a small number of hours; if the *Cow-*
143 *ley* [1981a] interpretation is correct, then evidence for such timescales should be present
144 when the magnetotail B_y component is correlated with the recent history of the IMF
145 B_y component. Other aspects of magnetospheric timescales have also been investigated.
146 *Cao et al.* [2013] investigated the timescales associated with energetic proton fluxes in the
147 central plasma sheet. They found a correlation with the magnitude of IMF B_z when the
148 IMF was southward, which was stronger if the IMF was lagged by 40-100 minutes. (No
149 correlation was found when the IMF was northward.) However, this is not a measure of
150 the Dungey cycle timescale; the authors interpret the delay as indicative of the timescale
151 for energy accumulation by addition of magnetic flux into the lobe (which does not corre-
152 spond to the full convection of a field line from the dayside to nightside reconnection sites).

153

154 Two recent studies have made more direct measurements of the timescales associated
155 with IMF penetration. *Rong et al.* [2015] carried out two case studies of events where
156 strong (5nT) variations in the IMF B_y component were identified with subsequent mag-
157 netotail plasma sheet B_y fluctuation in the same sense as the IMF. A lag time of 1-1.5

158 hours was found. An alternative approach was taken by *Zhang et al.* [2015], who carried
159 out a study of polar cap patches during a small geomagnetic storm. The patches were
160 tracked as they convected across the polar cap and returned at lower latitudes as part of
161 the Dungey cycle. The timescales taken for the polar cap patches to convect from noon to
162 midnight in MLT were approximately 1-2 hours, in agreement with *Rong et al.* [2015] but
163 slightly shorter than was found by *Fear and Milan* [2012a]. One possible explanation for
164 the apparent disagreement with the convection timescales from these three studies is the
165 differences in the IMF conditions. In the *Zhang et al.* [2015] and *Rong et al.* [2015] case
166 studies, the IMF B_z was negative or around zero respectively, whereas *Fear and Milan*
167 [2012a] were considering periods when transpolar arcs were present, and hence the IMF
168 was northward. The different IMF conditions in these studies indicate different levels of
169 dayside reconnection and hence different levels of driving of magnetospheric convection.
170 One would expect timescales for magnetospheric convection under northward IMF condi-
171 tions to be longer than when the IMF is southward.

172

173 If the *Cowley* [1981a] interpretation is correct, the above results suggest that a closer
174 correlation between the IMF B_y and plasma sheet B_y should be achieved with the inclu-
175 sion of a lag. Conversely, it has been suggested that field lines which reconnect to the
176 solar wind do not need to convect across the polar cap and undergo nightside reconnection
177 to introduce a B_y component into the neutral sheet. *Tenfjord et al.* [2015] has recently
178 suggested that when magnetospheric field lines undergo dayside reconnection, a perturba-
179 tion is introduced into the magnetosphere which forms a compressional MHD wave which
180 propagates through the magnetosphere much more quickly than field lines can convect.

181 They argue that the introduced perturbation has an asymmetry between the northern
182 and southern hemispheres that is in the same sense as the IMF; this means that a B_y
183 component can be introduced into the magnetotail by this process on a timescale of ap-
184 proximately 15 minutes.

185

186 In this study we extend the analysis of *Cao et al.* [2014] to include time dependencies;
187 in doing so we investigate statistically the timescales required for the IMF B_y component
188 to penetrate fully into the magnetosphere. In this way, we expect to be able to identify
189 the relative contributions of the mechanisms for penetration outlined by *Cowley* [1981a]
190 and *Tenfjord et al.* [2015]. If the timescales are determined to be mainly convection driven
191 processes, rather than pressure effects, then our observations will act as a means of iden-
192 tifying the timescales intrinsic to magnetospheric convection.

193

2. Instrumentation

194 In order to adopt the same approach as *Cao et al.* [2014], neutral sheet crossings were
195 identified in the data from Cluster 3 between 2001 and 2009. In order to identify the cross-
196 ings, we examined spin (4s) resolution data from the fluxgate magnetometer instrument
197 (FGM [*Balogh et al.*, 2001; *Gloag et al.*, 2010]). Data from the Cluster Ion Spectrometer
198 Hot Ion Analyser (CIS-HIA [*Rème et al.*, 2001; *Dandouras et al.*, 2010]) were used to
199 identify the presence or absence of fast flows in the plasma sheet. The OMNI database
200 was used to provide 1-minute resolution data on the solar wind conditions, specifically
201 the IMF vectors and solar wind dynamical pressure [*King and Papitashvili*, 2005].

202

3. Event Identification

203 In order to identify neutral sheet crossings, we identified reversals in the B_x compo-
 204 nent observed by Cluster 3 in the same spatial region as used by *Cao et al.* [2014]:
 205 $-14R_e > x_{GSM} > -19.6R_e$ (where $-19.6R_e$ is the apogee of the spacecraft) and $-9R_e <$
 206 $y_{GSM} < 11R_e$. The geocentric solar magnetospheric (GSM) coordinate system was used
 207 for this analysis as the x-z plane contains the dipole axis of the magnetosphere which
 208 removes internal mechanisms for addition of B_y in the plasma sheet. Excluding magne-
 209 totail B_x sign reversals which straddle data gaps of greater than 5 seconds, we identified
 210 6030 crossings, the locations of which are shown in Figure 1. As the neutral sheet is the
 211 boundary between the northern and southern hemispheres of the magnetotail, we expect
 212 the locations of the neutral sheet crossings to be around zero on the z-axis. Although
 213 there was not an explicit z-range criterion applied, most of the crossings fall in the range
 214 of $\pm 8R_e$ around zero on the z-axis. The exception is the small collection of points at $[-14,$
 215 $11, -15]R_e$, which are all the potential event detections identified from 2009. All of the
 216 identified events in 2009 occurred on the same orbit (11/10/2009 at 03:30 - 05:30UT).
 217 Examination of the in situ data from this orbit reveals that the spacecraft was situated
 218 in the magnetosheath, as indicated by the lower energies of the ion population (Figure
 219 2a, panel *i*) and the consistently fast ion velocity (Figure 2a, panel *v*) in the 2009 events
 220 compared to the corresponding panels in the sample data taken from 2001 (Figure 2b).
 221 Therefore, all events identified in 2009 were excluded, which leaves 5982 neutral sheet
 222 crossings for analysis. For each of the remaining neutral sheet crossings the magnetotail
 223 B_y component at the neutral sheet was determined by taking the mean of the B_y mea-
 224 surement immediately before and immediately after the B_x sign reversal. By taking only

225 B_y data from the neutral sheet, the addition of magnetotail B_y from magnetotail flaring
226 effects, as discussed in section 1, has been removed. Through a combination of adopting
227 GSM coordinates and taking data from the neutral sheet, we have eliminated the largest
228 sources of plasma sheet B_y other than by IMF penetration.

229

4. Investigation of Lag Times

230 As an initial step, to correlate the neutral sheet crossing B_y measurements with the
231 IMF B_y conditions, the IMF B_y component was averaged over an hour leading up to each
232 neutral sheet crossing (based on the 1-minute resolution OMNI data). These hour aver-
233 ages were then correlated with the measurements in the neutral sheet using the Pearson's
234 correlation coefficient, and the gradient from the least squares trend line is defined as the
235 penetration efficiency [Fairfield, 1979]. The penetration efficiency is calculated as it is a
236 measure of how closely the IMF and neutral sheet are related; if the IMF B_y component
237 penetrates into the magnetotail with 100% efficiency and with no other additions of B_y
238 in the neutral sheet, the gradient of the best fit trend line will become 1. The correlation
239 coefficient is a measure of how much scatter there is in the data from the best fit trend
240 line. When calculating these values for all of the neutral sheet crossings in our observing
241 region we find the correlation coefficient and penetration efficiency to be 0.63 and 0.56
242 respectively.

243

244 Once the B_y components from the neutral sheet crossings were correlated with in-
245 stantaneous measurements of the IMF B_y components, the effect of IMF B_y over longer
246 timescales was investigated. This was done by averaging the IMF B_y data over an hour

247 leading up to 10 minutes before the corresponding neutral sheet crossing and finding the
248 correlation coefficient and penetration efficiency of this lagged average of the IMF B_y
249 with the neutral sheet B_y . The 1 hour window (used to calculate the hour average) was
250 then moved progressively earlier in ten minute steps up to a maximum of 6 hours (i.e.
251 the longest delay considered related to a 1 hour window which ended 6 hours before the
252 neutral sheet crossing). In this way, we build up a picture of how the correlation coeffi-
253 cient and penetration efficiency evolves over that 6 hour time period. Figure 3 shows how
254 the correlation coefficient and penetration efficiency of the IMF into the magnetotail vary
255 over this 6 hour time period with the shaded regions highlighting the lag times reported
256 by previous studies (labelled). The values quoted above for the correlation coefficient
257 and penetration efficiency, with no lag applied to the solar wind data, correspond to the
258 values of the time series at the right-hand side of the figure. As the applied lag increases
259 (from right to left in the figure), the correlation coefficient peaks at a solar wind lag of
260 1 hour and then decreases and plateaus at 3 hours. The penetration efficiency shows a
261 clearer double peak feature with local maxima at about 2 hours and 3 hours 40 minutes.
262 The reason for this double feature is discussed in section 6. For context, we interpret the
263 penetration efficiency as a measure of how closely the IMF controls the magnetotail as
264 the closer the measurements of the IMF and magnetotail are the closer the penetration
265 efficiency gets to 1. We also interpret the correlation coefficient as a measure of scatter on
266 the data. In the following sections, we will show that as criteria based on the interplane-
267 tary conditions are applied, the traces of penetration efficiency and correlation coefficient
268 match more closely, indicating a higher degree of control (i.e. less scatter) as the data are

269 subsetted.

270

5. Event Filtering

271 In order to investigate the impact of magnetospheric convection on the timescales ev-
272 ident in Figure 3, we applied the criteria outlined by *Cao et al.* [2014] to the neutral
273 sheet crossings in order to exclude intervals of change in the magnetosphere (IMF B_z sign
274 changes, solar wind pressure pulses, and neutral sheet crossings that were observed at the
275 same time as fast flows in the magnetotail). Below we consider the effect of each of these
276 in turn.

277

5.1. IMF B_z sign changes

278 *Li et al.* [2011] suggested that a change in the sign of the IMF B_z component can in-
279 troduce a strong disturbance into the magnetosphere; therefore *Cao et al.* [2014] chose to
280 consider only periods of steady convection (at whatever rate). To do this, they excluded
281 events where the sign of the IMF B_z component changed in a 10 minute window, centred
282 on the time of the neutral sheet crossing (from 5 minutes before the crossing to 5 minutes
283 after).

284

285 Figure 4a shows how eliminating events during times of IMF B_z sign changes affects the
286 correlation and penetration efficiency as a function of lag time. Applying this criterion
287 emphasises the peak seen at around 4 hours but both peaks are still prominent. How-
288 ever, it generally has the effect of decreasing the penetration efficiency and correlation at

289 shorter lag times (less than 4 hours before the neutral sheet crossing), at which time both
290 then follow a similar trace to that observed in the unfiltered data. The peaks in this plot
291 occur at the same lag time as in the unfiltered data and have approximately the same value.

292

5.2. Solar wind Pressure Pulse

293 In order to exclude disturbances due to sudden changes in solar wind pressure, *Cao*
294 *et al.* [2014] also applied two solar wind pressure conditions based on absolute and rela-
295 tive changes in the pressure. Any crossing where there was a change in the solar wind
296 pressure that was greater than 2nPa or 50% within 5 minutes either side of the crossing
297 was excluded.

298

299 Figure 4b shows how eliminating events which coincided with relative or absolute
300 changes in the solar wind dynamical pressure of 2nPa (panel b1) or 50% (panel b2)
301 affects the lags. The peaks in each plot occur at the same lag time as in the unfiltered
302 data and have approximately the same value. The rest of the traces follow a similar trend
303 to that observed in the unfiltered data but at slightly lower values.

304

5.3. Fast Flows in the Magnetotail

305 The final condition applied by *Cao et al.* [2014] was the exclusion of neutral sheet cross-
306 ings for which there was a simultaneous observation of a fast flow, exceeding 100km s^{-1} ,
307 at the time of a neutral sheet crossing. Such a fast flow indicates the presence of a Bursty
308 Bulk Flow (BBF) which is associated with a dipolarization front [*Runov et al.*, 2009] and

309 hence is likely to be associated with a variation in the magnetic field due to the reconfig-
310 uration of the magnetosphere and is therefore not in a steady state. In this instance the
311 criterion was applied instantaneously (i.e. not within a 10 minute window centred on the
312 neutral sheet crossings).

313

314 Figure 4c shows the correlation and penetration over all lag times when fast flows in the
315 magnetotail are not present. Applying this criterion has acted to increase the correlation
316 at all lag times apart from close to the peak in Figure 3 at approximately 3 hours 30
317 minutes, where it has remained the same. The peak in correlation occurs at 1 hour 10
318 minutes with a value of 0.71 and the peak in penetration efficiency occurs at 3 hours with
319 a value of 0.72 although both traces now exhibit a very broad single peak. BBFs produce
320 strong variations in the local magnetic field and so eliminating them reduces the scat-
321 ter in the data, shown by the traces of penetration efficiency and correlation coefficient
322 matching more closely than in the unfiltered data in Figure 3.

323

324 In consistency with the analysis performed by *Cao et al.* [2014], each of the criteria were
325 combined as shown in Figure 5. It can be seen, during periods of a quiet magnetotail,
326 that the correlation is elevated for approximately 4 hours before a neutral sheet crossing
327 when the trace starts steadily decreasing; the penetration efficiency of the IMF into the
328 magnetotail peaks at around 4 hours before a neutral sheet crossing, then decreases at
329 around the same rate as the correlation coefficient.

330

6. Solar Wind Dependence

331 One would naturally expect the sign of the IMF B_z component to exert an influence on
332 the timescales associated with magnetospheric convection, and hence the distribution in
333 Figure 3. *Cao et al.* [2014] sought to account for this factor by excluding neutral sheet
334 crossings within 5 minutes of a sign change of the IMF B_z component. We propose,
335 however, that the time series of correlation and penetration efficiency should be more
336 closely controlled by the sign of the IMF B_z component rather than the presence or ab-
337 sence of sign changes. In order to filter separately periods of northward and southward
338 IMF, we defined each neutral sheet crossing as occurring during a period of “generally
339 northward” or “generally southward” IMF. “Generally northward” was defined to occur
340 when more than 60% of the 1-minute IMF B_z data over 2 hours leading up to the neutral
341 sheet crossing was greater than $1nT$, or less than $-3nT$ for “generally southward” IMF.
342 (For clarity, we expect reconnection to take place under northward IMF conditions when
343 the magnitude of IMF B_y component dominates the IMF B_z component [*Freeman et al.*,
344 1993].) The asymmetry in the criteria provides the best balance between being as strict as
345 possible about which events were included without removing so many as to lose statistical
346 validity. Figure 6 shows that periods of generally negative IMF B_z give a relatively prompt
347 response of approximately 1 hour, compared to the time series plot for positive IMF B_z
348 where the correlation and penetration efficiency are both elevated for over 4 hours before
349 the neutral sheet crossing. It can also be seen in Figure 6 that the correlation coefficient
350 matches the penetration efficiency much more closely than in Figure 3; we propose that
351 this is due to the criteria eliminating sources of scatter.

352

353 As part of the hypothesis that the lag time would depend on dayside reconnection
354 rate, the other factor which has to be taken into account is the solar wind velocity, as
355 reflected by empirical expressions for the dayside reconnection rate [*Newell et al.*, 2007;
356 *Milan et al.*, 2012; *Borovsky*, 2013]. If the solar wind is fast then there will be a high
357 arrival rate of IMF field lines at the magnetopause and therefore for a given reconnection
358 efficiency, more field lines will have the opportunity to undergo reconnection; this in turn
359 drives magnetospheric convection more rapidly than the opposite situation of slow solar
360 wind conditions. Where the solar wind is slow the IMF field lines are arriving at a slower
361 rate and so dayside reconnection rate decreases, also decreasing the amount of driving
362 in the magnetosphere. We therefore expect a more prompt response for fast solar wind
363 speeds due to the increased driving of magnetospheric convection, and a slower timescale
364 for slower solar wind speeds. We test this hypothesis by defining crossings as being as-
365 sociated with periods of “generally slow” or “generally fast” solar wind speeds if more
366 than 60% of the 1-minute averaged solar wind velocity measurements from the 2 hours
367 leading up to the neutral sheet crossing were less than 400km s^{-1} or greater than 440km
368 s^{-1} respectively. Again, boundaries are chosen so as not to eliminate too many neutral
369 sheet crossings so that the statistical significance of the analysis remains high.

370

371 The results in Figure 7 show that for crossings associated with generally fast solar wind
372 speeds, the correlation was elevated for two hours immediately before the neutral sheet
373 crossing whereas the correlation was elevated for approximately 4 hours immediately be-
374 fore the crossings associated with slow solar wind speeds. The differences are starker in
375 the behaviour of the penetration efficiency, which peaks at about 2 hours before the cross-

ings for the fast solar wind speed events, and about 4 hours before for the slow solar wind
events. The plot for generally fast solar wind events shows a secondary peak at around 4
hours which is only present in the penetration efficiency but coincides with a plateau in
the correlation coefficient which is otherwise gradually decreasing. We conclude that this
secondary feature is due to the threshold for “generally fast” solar wind not being set high
enough, however setting this value any higher rapidly decreases the statistical validity of
the result.

In order to investigate if the peak in lag time depends on dayside reconnection rate, as
predicted by empirical expressions, every combination of the IMF B_z and solar wind speed
criteria was applied to the dataset of neutral sheet crossings, which is shown in Figure 8.
We would expect the reconnection rate to be highest and hence the convection timescale
fastest if IMF B_z is negative and the solar wind is fast. If the IMF B_z is positive and the
solar wind speed is slow, we expect the reconnection rate to be slow and therefore the
response time of the magnetotail also to be slow. The other combinations are expected to
lie somewhere in-between these two extreme conditions. The bottom right panel of Figure
8 shows that this is the case, with conditions most favourable for reconnection giving a
response time of less than an hour, which then drops away after two hours. Where recon-
nection is least favourable, shown in the top left panel of Figure 8, there is a peak in the
correlation and penetration between 3-5 hours. The other two panels in this Figure show
traces of penetration efficiency and correlation that peak in between these two extremes
as predicted. By applying the solar wind speed and IMF B_z criteria we observe a much
closer agreement between the traces of penetration efficiency and correlation coefficient

399 which, as described earlier, indicates that scatter in the data has been reduced. These
400 observations in Figure 8 fit well with the suggested mechanism that dayside reconnection
401 rate drives magnetospheric convection and therefore influences how long it takes for the
402 IMF to penetrate into closed field lines in the magnetotail.

403

7. Discussion

404 By taking magnetotail B_Y data from all neutral sheet crossings that occurred during
405 the observing region defined by *Cao et al.* [2014] and correlating these measurements with
406 IMF B_y data at increasing lag times, peaks in the correlation and penetration efficiency
407 are observed, as seen in Figure 3. The locations at which previous studies have observed
408 lag times coincide with peaks in the penetration efficiency and similar features in the
409 correlation coefficient series.

410

411 To investigate what could be causing multiple timescales, we applied the criteria defined
412 in *Cao et al.* [2014] to select neutral sheet crossing events that occurred during times of
413 a quiet magnetosphere. Applying the same range of lag times to the solar wind data as
414 was used for unfiltered events, a greater penetration of the IMF B_y component into the
415 B_y component of the magnetotail is observed when a lag of approximately 4 hours is ap-
416 plied (Figure 5). The correlation coefficient is elevated for 4 hours before a neutral sheet
417 crossing before decreasing, in agreement with the timescales observed in the penetration
418 efficiency.

419

420 One of the criteria defined in *Cao et al.* [2014] was for no sign changes in IMF B_z . *Cao*
421 *et al.* [2014] proposed this as *Keika et al.* [2008] and *Li et al.* [2011] have reported that
422 initiating or halting dayside reconnection can introduce a perturbation in the magneto-
423 sphere which could affect the B_y component measured in the magnetotail. We propose,
424 however, that the sign of the IMF B_z component has a greater effect on timescales than
425 the presence of sign changes, because the sign of IMF B_z largely controls the presence
426 or absence of dayside reconnection, and hence the driving of the magnetosphere. We hy-
427 pothesise that when magnetospheric convection is being driven, a more prompt timescale
428 should be observed than when magnetospheric convection is stalled.

429
430 By taking northward IMF conditions to be when dayside reconnection is less favourable,
431 it can be seen in the left plot of Figure 6 that the observations provide evidence for the
432 hypothesis that a quiet magnetotail requires a longer time for the IMF to penetrate and
433 then be removed from the magnetotail. The observed 4 hour lag time is consistent with
434 the value found by *Fear and Milan* [2012a] (3-4 hours) when looking at the formation of
435 transpolar arcs, which require northward IMF conditions. By taking events that occurred
436 after a two hour period of generally southward IMF conditions, a much more prompt peak
437 is observed in both the correlation coefficient and penetration efficiency at approximately
438 40-60 minutes (right plot in Figure 6) which is consistent with the values found by *Rong*
439 *et al.* [2015] and *Zhang et al.* [2015] who were looking at events during periods of south-
440 ward IMF conditions. The observed time lag during periods of southward IMF conditions
441 is also consistent with reported timescales associated with substorms such as the previous
442 superposed epoch analysis by *Milan et al.* [2010] who showed that for 2000 substorms the

443 time lag between there being a southward turning of the IMF relative to substorm onset
444 was up to 2 hours; also, observations by *Østgaard et al.* [2005] found that magnetotail
445 twisting started to be influenced only 10 minutes after the arrival of IMF B_y . This window
446 of 10 minutes to 2 hours from *Østgaard et al.* [2005] and *Milan et al.* [2010] respectively
447 is consistent with an elevated correlation and penetration efficiency in the right panel
448 of Figure 6 and also the hypothesis that during periods of high magnetospheric driving
449 caused by a high dayside reconnection rate the timescale for magnetospheric convection,
450 and therefore timescales for the penetration of the IMF B_y component into the magne-
451 tosphere, is low. The difference in timescales between southward and northward IMF
452 conditions (shown in Figure 6) allows us to draw a synthesis between the two phenomena
453 of substorms [*Milan et al.*, 2010] and transpolar arcs [*Fear and Milan*, 2012a], both of
454 which are caused by magnetotail reconnection but under IMF conditions that are prefer-
455 ential for high and low magnetospheric driving respectively and have exhibited timescales
456 consistent with those found in this study for their required IMF conditions.

457

458 The hypothesis was further tested by examining how timescales depend on the solar
459 wind speed. An effect might be expected, as the dayside reconnection rate is partly
460 controlled by the solar wind speed [*Newell et al.*, 2007; *Milan et al.*, 2012; *Borovsky*,
461 2013]. As described in the previous section, we expect slow solar wind to indicate times
462 of a low dayside reconnection rate and therefore a quiet magnetosphere, requiring longer
463 timescales for IMF penetration. Oppositely, during times of fast solar wind speed, the
464 dayside reconnection rate will be higher and therefore magnetospheric convection will be
465 more active giving a more prompt response time of the magnetosphere to the IMF. In a

466 similar way to our approach of examining periods of “generally southward” and “generally
467 northward” IMF B_z conditions, the solar wind was filtered to find times of “generally fast”
468 or “generally slow” solar wind over two hours leading up to the neutral sheet crossing.
469 Figure 7 shows that for slow solar wind, a long timescale is observed of approximately 4
470 hours where the correlation coefficient is elevated, and the penetration efficiency peaks at
471 that time. This timescale is similar to that observed for northward IMF conditions, when
472 dayside reconnection is also less favourable. As expected, fast solar wind conditions ex-
473 hibit a much more prompt response time of approximately 2 hours where the penetration
474 efficiency peaks and the correlation coefficient is elevated up to this lag time.

475

476 The plots from Figure 8 show that by selecting neutral sheet crossings that occurred un-
477 der certain solar wind conditions related to the dayside reconnection rate, a change in the
478 response time of the neutral sheet is observed. When the expected dayside reconnection
479 rate is low (Figure 8, top left panel), a long lag time is again observed which is consistent
480 with the previous result in this study and the result found by *Fear and Milan* [2012a].
481 When the dayside reconnection rate is high, however (Figure 8, bottom right panel), a
482 much more prompt response is found where the penetration efficiency exhibits a broad
483 peak at approximately 40 minutes to 2 hours before sharply decreasing; the correlation
484 coefficient indicates that there is the least amount of scatter on the data at approximately
485 40 minutes and remains elevated for up to 2 hours, which is more consistent with values
486 found by *Rong et al.* [2015] and *Zhang et al.* [2015].

487

488 *Tenfjord et al.* [2015] suggest that when dayside reconnection occurs during conditions
489 of IMF $B_y \neq 0$ there are asymmetries between the density of field lines in the dusk/dawn
490 sectors of the northern and southern hemispheres. This asymmetric addition of flux im-
491 parts a pressure upon the magnetotail which causes it to reconfigure to a state which is
492 consistent with the IMF including its B_y component. Simulations run by *Tenfjord et al.*
493 [2015] have estimated that this reconfiguration will take approximately 15 minutes and,
494 if significant, should also correspond to the lag time which gives rise to peaks in the pen-
495 etration efficiency and correlation coefficient; however our results are not consistent with
496 this scenario. Whilst there may be an MHD pressure wave that causes the magnetotail
497 to reconfigure to IMF conditions more rapidly than by the convection of field lines, its
498 significance (compared to a B_y component induced from field line convection) is low and
499 cannot be seen above the background correlation which we propose is due to the finite
500 timescales by which the solar wind varies. Oppositely, observations have been reported
501 that the IMF B_y component has to have either positive or negative values for up to a day
502 to fully have an effect on the onset MLT location of substorms [*Milan et al.*, 2010]; simi-
503 larly, *Grocott and Milan* [2014] have reported that the shape of the ionospheric convection
504 patterns are still being altered after 10 hours when there has been a persistent IMF B_y
505 component. The mechanism behind these longer timescales is unknown.

506

507 It has been estimated that the timescale for the penetration of the IMF into the mag-
508 netotail should take of the order of hours [*Dungey*, 1965; *Cowley*, 1981b; *Fear and Milan*,
509 2012a], based on the time taken for the ionospheric end of an open field line to cross the
510 polar cap. In Table 1, we develop this idea further by using the distribution of polar cap

511 areas reported by *Milan et al.* [2007] and a distribution of polar cap convection speed
512 vectors observed near the pole in the midnight sector [*Grocott et al.*, 2009] by Super-
513 DARN [*Greenwald et al.*, 1995; *Chisham et al.*, 2007]. The ionospheric convection speeds
514 were calculated from the 2-dimensional ionospheric velocity vectors which were derived
515 using the map potential technique [*Ruohoniemi and Baker*, 1998] within an $\sim 500 \times 500$ km
516 box, centred at a latitude of $\sim 83^\circ$ at midnight MLT (magnetic local time). The precise
517 location of the box is scaled to the zero potential boundary, and the precise size of the
518 box scales accordingly. The reader is referred to *Grocott et al.* [2009] for a more detailed
519 description of the statistical database used (the box in question is no. 33 from Fig. 2 in
520 their paper). The speeds used are averages of at least two measurements located within
521 the box; one average speed value was calculated for each 2 minute interval between 1999
522 and 2006 for which there were at least two points of ionospheric scatter in the box. Fig-
523 ure 9 (left histogram) shows the occurrence of ionospheric convection speeds binned in
524 50 m s^{-1} increments; in this figure, any flows where the corresponding vector has a sun-
525 ward component have been removed. The histogram on the right-hand side of Figure 9
526 shows occurrence of polar cap diameters binned in 500 km increments, converted from the
527 areas reported in Figure 3 of *Milan et al.* [2007]. Using the mode field line convection
528 speed of 330 m s^{-1} and the mode polar cap area of $1.1 \times 10^{13} \text{ m}^2$ (Figure 9) [*Milan et al.*,
529 2003, 2007, 2009], giving a cross polar cap distance of approximately 3800 km, we estimate
530 the time taken for a field line to be transported through the lobe to be approximately 3
531 hours (Table 1, centre cell). This estimate compares well with *Cowley* [1981b] and *Fear*
532 *and Milan* [2012a] estimates, based on similar calculations. By taking the lower and upper
533 quartiles of convection speeds (240 m s^{-1} and 440 m s^{-1} respectively), and polar cap areas

534 (9.4 and 14×10^{12} km² respectively – Figure 9), Table 1 shows how the timescale for con-
535 vection of field lines from the dayside magnetopause to the lobe-plasma sheet boundary
536 might be expected to vary from approximately 2-5 hours. As our observations are taken
537 from the neutral sheet we expect these calculations to be a slight underestimate; this is
538 because the spacecraft measures the neutral sheet Earthward of the tail x-line and so the
539 field lines have convected further (and for longer) than we have accounted for in the calcu-
540 lation. It can be seen that the estimate for the upper limit of magnetospheric convection
541 always contains the peak in correlation and penetration in all lag time figures (Figures 3-8).

542

8. Conclusion

543 In this study we have presented statistical evidence for the timescales associated with
544 the penetration of the IMF into the neutral sheet. We find two distinct timescales close
545 to 2 hours and 4 hours which are consistent with estimates for timescales found by previ-
546 ous studies for southward and northward IMF respectively. Events were then filtered by
547 whether the event occurred during “generally northward” or “generally southward” IMF
548 conditions. When the IMF was “generally southward” the response time of the plasma
549 sheet to the penetration of IMF B_y was around 1-2 hours; when the IMF was “generally
550 northward”, the plasma sheet was correlated for up to 5 hours. During “generally fast”
551 solar wind conditions there was a response time of ~ 2 hours for the IMF B_y to enter
552 the plasma sheet, and under “generally slow” solar wind conditions the plasma sheet was
553 observed to correlate with the IMF for up to 4 hours beforehand, with a peak in the
554 penetration efficiency at ~ 4 hours.

555

556 By applying criteria to the sign on the IMF B_z component and the solar wind speed
557 we found that the relative heights of the peaks in correlation and penetration efficiency
558 changed based on the strength of the magnetospheric driving. By combining the IMF B_z
559 and solar wind speed criteria we expect the penetration timescale to vary if penetration
560 is controlled by dayside reconnection rate, as dayside reconnection is the primary mecha-
561 nism behind magnetospheric driving. We found that when the dayside reconnection rate
562 is high (therefore magnetospheric driving is high) there is a much more rapid response of
563 the neutral sheet to changes in the IMF conditions of the order of 1-2 hours; conversely,
564 when the dayside reconnection rate is low (low magnetospheric driving) there was a much
565 longer timescale associated with IMF penetration of the order of 3-5 hours. Our observed
566 timescales are consistent with the range expected from calculations based on arguments
567 by *Dungey* [1965] (see our Table 1).

568

569 **Acknowledgments.**

570 Cluster data were obtained from the Cluster Active Archive (<http://caa.estec.esa.int/caa/>)

571 The OMNI data were obtained from the SPDF OMNIWeb interface at <http://omniweb.gsfc.nasa.gov>

572 SDB was supported by Science and Technology Facilities Council (STFC) studentship

573 ST/M503794/1

574 RCF was supported by STFC Ernest Rutherford Fellowship ST/K004298/2.

575 AG was supported by STFC grant number ST/M001059/1.

576 SEM was supported by STFC grant ST/N000749/1. The work at the Birkeland Centre

577 for Space Centre, University of Bergen, Norway, was supported by the Research Council

578 of Norway/CoE under contract 223252/F50.

579

580 RCF would like to thank Oscar Miles and Natasha Dell for their preliminary work on
581 this project.

582 SDB would also like to thank Paul Tenfjord from the University of Bergen for providing
583 feedback and his insight.

References

- 584 Balogh, A., C. M. Carr, M. H. Acuña, M. W. Dunlop, T. J. Beek, P. Brown, K.-H.
585 Fornaçon, E. Georgescu, K.-H. Glassmeier, J. Harris, G. Musmann, T. Oddy, and
586 K. Schwingenschuh (2001), The Cluster Magnetic Field Investigation: overview of
587 in-flight performance and initial results, *Annales Geophysicae*, *19*, 1207–1217, doi:
588 10.5194/angeo-19-1207-2001.
- 589 Borovsky, J. E. (2013), Physical improvements to the solar wind reconnection control func-
590 tion for the Earth’s magnetosphere, *Journal of Geophysical Research: Space Physics*,
591 *118*(5), 2113–2121, doi:10.1002/jgra.50110.
- 592 Cao, J., A. Duan, H. Reme, and I. Dandouras (2013), Relations of the energetic proton
593 fluxes in the central plasma sheet with solar wind and geomagnetic activities, *Journal*
594 *of Geophysical Research (Space Physics)*, *118*, 7226–7236, doi:10.1002/2013JA019289.
- 595 Cao, J., A. Duan, M. Dunlop, X. Wei, and C. Cai (2014), Dependence of IMF B_y penetra-
596 tion into the neutral sheet on IMF B_z and geomagnetic activity, *Journal of Geophysical*
597 *Research (Space Physics)*, *119*, 5279–5285, doi:10.1002/2014JA019827.

- 598 Chisham, G., M. Lester, S. E. Milan, M. P. Freeman, W. A. Bristow, A. Grocott,
599 K. A. McWilliams, J. M. Ruohoniemi, T. K. Yeoman, P. L. Dyson, R. A. Greenwald,
600 T. Kikuchi, M. Pinnock, J. P. S. Rash, N. Sato, G. J. Sofko, J.-P. Villain, and A. D. M.
601 Walker (2007), A decade of the Super Dual Auroral Radar Network (SuperDARN):
602 scientific achievements, new techniques and future directions, *Surveys in Geophysics*,
603 *28*, 33–109, doi:10.1007/s10712-007-9017-8.
- 604 Cowley, S. W. H. (1981a), Magnetospheric asymmetries associated with the y-component
605 of the IMF, *Planetary and Space Science*, *29*, 79–96, doi:10.1016/0032-0633(81)90141-0.
- 606 Cowley, S. W. H. (1981b), Magnetospheric and ionospheric flow and the interplane-
607 tary magnetic field, in *Physical basis of the Ionosphere in the Solar-Terrestrial System*,
608 AGARD CP-295, pp. 4.1–4.14.
- 609 Dandouras, I., A. Barthe, E. Penou, S. Brunato, H. Rème, L. M. Kistler, M. B. Bavassano-
610 Cattaneo, and A. Blagau (2010), Cluster Ion Spectrometry (CIS) Data in the Cluster
611 Active Archive (CAA), *Astrophysics and Space Science Proceedings*, *11*, 51–72, doi:
612 10.1007/978-90-481-3499-13.
- 613 Dungey, J. W. (1961), Interplanetary Magnetic Field and the Auroral Zones, *Physical*
614 *Review Letters*, *6*, 47–48, doi:10.1103/PhysRevLett.6.47.
- 615 Dungey, J. W. (1965), The Length of the Magnetospheric Tail, *J. Geophys. Res.*, , *70*,
616 1753–1753, doi:10.1029/JZ070i007p01753.
- 617 Fairfield, D. H. (1979), On the average configuration of the geomagnetic tail, *J. Geophys.*
618 *Res.*, , *84*, 1950–1958, doi:10.1029/JA084iA05p01950.
- 619 Fear, R. C., and S. E. Milan (2012a), The IMF dependence of the local time of transpolar
620 arcs: Implications for formation mechanism, *Journal of Geophysical Research (Space*

- 621 *Physics*), 117, A03213, doi:10.1029/2011JA017209.
- 622 Fear, R. C., and S. E. Milan (2012b), Ionospheric flows relating to transpolar arc
623 formation, *Journal of Geophysical Research (Space Physics)*, 117, A09230, doi:
624 10.1029/2012JA017830.
- 625 Frank, L. A., J. D. Craven, J. L. Burch, and J. D. Winningham (1982), Polar views of the
626 earth's aurora with dynamics explorer, *Geophysical Research Letters*, 9(9), 1001–1004,
627 doi:10.1029/GL009i009p01001.
- 628 Freeman, M. P., C. J. Farrugia, L. F. Burlaga, M. R. Hairston, M. E. Greenspan, J. M.
629 Ruohoniemi, and R. P. Lepping (1993), The interaction of a magnetic cloud with the
630 Earth - Ionospheric convection in the Northern and Southern Hemispheres for a wide
631 range of quasi-steady interplanetary magnetic field conditions, *J. Geophys. Res.*, , 98,
632 7633–7655, doi:10.1029/92JA02350.
- 633 Gloag, J. M., E. A. Lucek, L.-N. Alconcel, A. Balogh, P. Brown, C. M. Carr, C. N.
634 Dunford, T. Oddy, and J. Soucek (2010), FGM Data Products in the CAA, in *The*
635 *Cluster Active Archive - Studying the Earth's Space Plasma Environment*, edited by
636 H. Laakso, M. Taylor, and P. Escoubet, pp. 109–128, Springer Netherlands, Dordrecht,
637 doi:10.1007/978-90-481-3499-1/7.
- 638 Greenwald, R. A., K. B. Baker, J. R. Dudeney, M. Pinnock, T. B. Jones, E. C.
639 Thomas, J.-P. Villain, J.-C. Cerisier, C. Senior, C. Hanuise, R. D. Hunsucker, G. Sofko,
640 J. Koehler, E. Nielsen, R. Pellinen, A. D. M. Walker, N. Sato, and H. Yamagishi (1995),
641 Darn/Superdarn: A Global View of the Dynamics of High-Latitude Convection, *ssr*,
642 71, 761–796, doi:10.1007/BF00751350.

- 643 Grocott, A., and S. E. Milan (2014), The influence of IMF clock angle timescales on the
644 morphology of ionospheric convection, *Journal of Geophysical Research (Space Physics)*,
645 *119*, 5861–5876, doi:10.1002/2014JA020136.
- 646 Grocott, A., J. A. Wild, S. E. Milan, and T. K. Yeoman (2009), Superposed epoch analysis
647 of the ionospheric convection evolution during substorms: onset latitude dependence,
648 *Annales Geophysicae*, *27*, 591–600, doi:10.5194/angeo-27-591-2009.
- 649 Hau, L.-N., and G. M. Erickson (1995), Penetration of the interplanetary magnetic
650 field B_y into Earth’s plasma sheet, *J. Geophys. Res.*, , *100*, 21,745–21,752, doi:
651 10.1029/95JA01935.
- 652 Hilmer, R. V., and G.-H. Voigt (1987), The effects of magnetic $B(y)$ compo-
653 nent on geomagnetic tail equilibria, *J. Geophys. Res.*, , *92*, 8660–8672, doi:
654 10.1029/JA092iA08p08660.
- 655 Kaymaz, Z., G. L. Siscoe, J. G. Luhmann, R. P. Lepping, and C. T. Russell (1994),
656 Interplanetary magnetic field control of magnetotail magnetic field geometry: IMP 8
657 observations, *J. Geophys. Res.*, , *99*, 11,113–11,126, doi:10.1029/94JA00300.
- 658 Keika, K., R. Nakamura, W. Baumjohann, A. Runov, T. Takada, M. Volwerk, T. L. Zhang,
659 B. Klecker, E. A. Lucek, C. Carr, H. Rème, I. Dandouras, M. André, and H. Frey (2008),
660 Response of the inner magnetosphere and the plasma sheet to a sudden impulse, *Journal*
661 *of Geophysical Research (Space Physics)*, *113*, A07S35, doi:10.1029/2007JA012763.
- 662 King, J. H., and N. E. Papitashvili (2005), Solar wind spatial scales in and comparisons of
663 hourly Wind and ACE plasma and magnetic field data, *Journal of Geophysical Research*
664 *(Space Physics)*, *110*, A02104, doi:10.1029/2004JA010649.

- 665 Li, L. Y., J. B. Cao, G. C. Zhou, T. L. Zhang, D. Zhang, I. Dandouras, H. Rème,
666 and C. M. Carr (2011), Multiple responses of magnetotail to the enhancement and
667 fluctuation of solar wind dynamic pressure and the southward turning of interplanetary
668 magnetic field, *Journal of Geophysical Research (Space Physics)*, *116*(15), A12223, doi:
669 10.1029/2011JA016816.
- 670 Milan, S. E., M. Lester, S. W. H. Cowley, K. Oksavik, M. Brittnacher, R. A. Greenwald,
671 G. Sofko, and J.-P. Villain (2003), Variations in the polar cap area during two substorm
672 cycles, *Annales Geophysicae*, *21*, 1121–1140, doi:10.5194/angeo-21-1121-2003.
- 673 Milan, S. E., B. Hubert, and A. Grocott (2005), Formation and motion of a transpolar
674 arc in response to dayside and nightside reconnection, *Journal of Geophysical Research*
675 (*Space Physics*), *110*, A01212, doi:10.1029/2004JA010835.
- 676 Milan, S. E., G. Provan, and B. Hubert (2007), Magnetic flux transport in the Dungey
677 cycle: A survey of dayside and nightside reconnection rates, *Journal of Geophysical*
678 *Research (Space Physics)*, *112*, A01209, doi:10.1029/2006JA011642.
- 679 Milan, S. E., J. Hutchinson, P. D. Boakes, and B. Hubert (2009), Influences on the radius
680 of the auroral oval, *Annales Geophysicae*, *27*, 2913–2924, doi:10.5194/angeo-27-2913-
681 2009.
- 682 Milan, S. E., A. Grocott, and B. Hubert (2010), A superposed epoch analysis of auroral
683 evolution during substorms: Local time of onset region, *Journal of Geophysical Research*
684 (*Space Physics*), *115*, A00I04, doi:10.1029/2010JA015663.
- 685 Milan, S. E., J. S. Gosling, and B. Hubert (2012), Relationship between interplanetary
686 parameters and the magnetopause reconnection rate quantified from observations of the
687 expanding polar cap, *Journal of Geophysical Research (Space Physics)*, *117*, A03226,

688 doi:10.1029/2011JA017082.

689 Moses, J. J., N. U. Crooker, D. J. Gorney, and G. L. Siscoe (1985), High-latitude con-
690 vection on open and closed field lines for large IMF $B(y)$, *J. Geophys. Res.*, , 90, 11,
691 doi:10.1029/JA090iA11p11078.

692 Nagai, T. (1987), Interplanetary magnetic field B_y effects on the magnetic field at syn-
693 chronous orbit, *J. Geophys. Res.*, , 92, 11,215–11,220, doi:10.1029/JA092iA10p11215.

694 Newell, P. T., D. G. Sibeck, and C.-I. Meng (1995), Penetration of the interplanetary
695 magnetic field B_y magnetosheath plasma into the magnetosphere: Implications for
696 the predominant magnetopause merging site, *J. Geophys. Res.*, , 100, 235–243, doi:
697 10.1029/94JA02632.

698 Newell, P. T., T. Sotirelis, K. Liou, C.-I. Meng, and F. J. Rich (2007), A nearly universal
699 solar wind-magnetosphere coupling function inferred from 10 magnetospheric state vari-
700 ables, *Journal of Geophysical Research: Space Physics*, 112, doi:10.1029/2006JA012015,
701 A01206.

702 Nishida, A., and T. Ogino (1998), Convection and Reconnection in the Earth's Magneto-
703 tail, *Washington DC American Geophysical Union Geophysical Monograph Series*, 105,
704 61.

705 Nishida, A., T. Mukai, T. Yamamoto, Y. Saito, S. Kokubun, and K. Maezawa (1995),
706 GEOTAIL observation of magnetospheric convection in the distant tail at 200 R_E in
707 quiet times, *J. Geophys. Res.*, , 100, 23,663–23,676, doi:10.1029/95JA02519.

708 Nishida, A., T. Mukai, T. Yamamoto, S. Kokubun, and K. Maezawa (1998), A unified
709 model of the magnetotail convection in geomagnetically quiet and active times, *J. Geo-
710 phys. Res.*, , 103, 4409–4418, doi:10.1029/97JA01617.

711 Østgaard, N., N. A. Tsyganenko, S. B. Mende, H. U. Frey, T. J. Immel, M. Fillingim,
712 L. A. Frank, and J. B. Sigwarth (2005), Observations and model predictions of substorm
713 auroral asymmetries in the conjugate hemispheres, *Geophys. Res. Lett.*, , *32*, L05111,
714 doi:10.1029/2004GL022166.

715 Petrukovich, A. A. (2009), Dipole tilt effects in plasma sheet B_y : statistical model and
716 extreme values, *Annales Geophysicae*, *27*, 1343–1352, doi:10.5194/angeo-27-1343-2009.

717 Petrukovich, A. A. (2011), Origins of plasma sheet B_y , *Journal of Geophysical Research*
718 (*Space Physics*), *116*, A07217, doi:10.1029/2010JA016386.

719 Rème, H., C. Aoustin, J. M. Bosqued, I. Dandouras, B. Lavraud, J. A. Sauvaud, A. Barthe,
720 J. Bouyssou, T. Camus, O. Coeur-Joly, A. Cros, J. Cuvilo, F. Ducay, Y. Garbarowitz,
721 J. L. Medale, E. Penou, H. Perrier, D. Romefort, J. Rouzaud, C. Vallat, D. Alcaydé,
722 C. Jacquy, C. Mazelle, C. D’Uston, E. Möbius, L. M. Kistler, K. Crocker, M. Granoff,
723 C. Mouikis, M. Popecki, M. Vosbury, B. Klecker, D. Hovestadt, H. Kucharek, E. Kuen-
724 neth, G. Paschmann, M. Scholer, N. Sckopke, E. Seidenschwang, C. W. Carlson, D. W.
725 Curtis, C. Ingraham, R. P. Lin, J. P. McFadden, G. K. Parks, T. Phan, V. Formisano,
726 E. Amata, M. B. Bavassano-Cattaneo, P. Baldetti, R. Bruno, G. Chionchio, A. di Lel-
727 lis, M. F. Marcucci, G. Pallochia, A. Korth, P. W. Daly, B. Graeve, H. Rosenbauer,
728 V. Vasyliunas, M. McCarthy, M. Wilber, L. Eliasson, R. Lundin, S. Olsen, E. G. Shelley,
729 S. Fuselier, A. G. Ghielmetti, W. Lennartsson, C. P. Escoubet, H. Balsiger, R. Friedel,
730 J.-B. Cao, R. A. Kovrazhkin, I. Papamastorakis, R. Pellat, J. Scudder, and B. Sonnerup
731 (2001), First multispacecraft ion measurements in and near the Earth’s magnetosphere
732 with the identical Cluster ion spectrometry (CIS) experiment, *Annales Geophysicae*, *19*,
733 1303–1354, doi:10.5194/angeo-19-1303-2001.

- 734 Rong, Z. J., A. T. Y. Lui, W. X. Wan, Y. Y. Yang, C. Shen, A. A. Petrukovich, Y. C.
735 Zhang, T. L. Zhang, and Y. Wei (2015), Time delay of interplanetary magnetic field
736 penetration into Earth's magnetotail, *Journal of Geophysical Research: Space Physics*,
737 *120*(5), 3406–3414, doi:10.1002/2014JA020452, 2014JA020452.
- 738 Runov, A., V. Angelopoulos, M. I. Sitnov, V. A. Sergeev, J. Bonnell, J. P. McFad-
739 den, D. Larson, K.-H. Glassmeier, and U. Auster (2009), Themis observations of
740 an earthward-propagating dipolarization front, *Geophysical Research Letters*, *36*, doi:
741 10.1029/2009GL038980, 114106.
- 742 Ruohoniemi, J. M., and K. B. Baker (1998), Large-scale imaging of high-latitude con-
743 vection with Super Dual Auroral Radar Network HF radar observations, *Journal of*
744 *Geophysical Research*, *103*, 20,797–20,811, doi:10.1029/98JA01288.
- 745 Sergeev, V. A. (1987), Penetration of the By component of the IMF into the magnetotail,
746 *Geomagnetism and Aeronomy*, *27*, 612–615.
- 747 Tenfjord, P., N. Østgaard, K. Snekvik, K. M. Laundal, J. P. Reistad, S. Haaland, and
748 S. E. Milan (2015), How the IMF B_y induces a B_y component in the closed magne-
749 tosphere and how it leads to asymmetric currents and convection patterns in the two
750 hemispheres, *Journal of Geophysical Research (Space Physics)*, *120*, 9368–9384, doi:
751 10.1002/2015JA021579.
- 752 Tsurutani, B. T., E. J. Smith, D. E. Jones, R. P. Lepping, and D. G. Sibeck (1984), The
753 relationship between the IMF B_y and the distant tail (150–238 R_e) lobe and plasmashet
754 B_y fields, *Geophys. Res. Lett.*, *11*, 1082–1085, doi:10.1029/GL011i010p01082.
- 755 Voigt, G.-H., and R. V. Hilmer (1987), The influence of the IMF B_y component on the
756 Earth's magneto-hydrostatic magnetotail, in *Magnetotail Physics*, edited by A. T. Y.

757 Lui and S.-I. Akasofu, pp. 91–97.

758 Wing, S., P. T. Newell, D. G. Sibeck, and K. B. Baker (1995), A large statistical study
759 of the entry of interplanetary magnetic field Y-component into the magnetosphere,
760 *Geophys. Res. Lett.*, , 22, 2083–2086, doi:10.1029/95GL02261.

761 Zhang, Q.-H., M. Lockwood, J. C. Foster, S.-R. Zhang, B.-C. Zhang, I. W. McCrea,
762 J. Moen, M. Lester, and J. M. Ruohoniemi (2015), Direct observations of the full
763 Dungey convection cycle in the polar ionosphere for southward interplanetary magnetic
764 field conditions, *Journal of Geophysical Research (Space Physics)*, 120, 4519–4530, doi:
765 10.1002/2015JA021172.

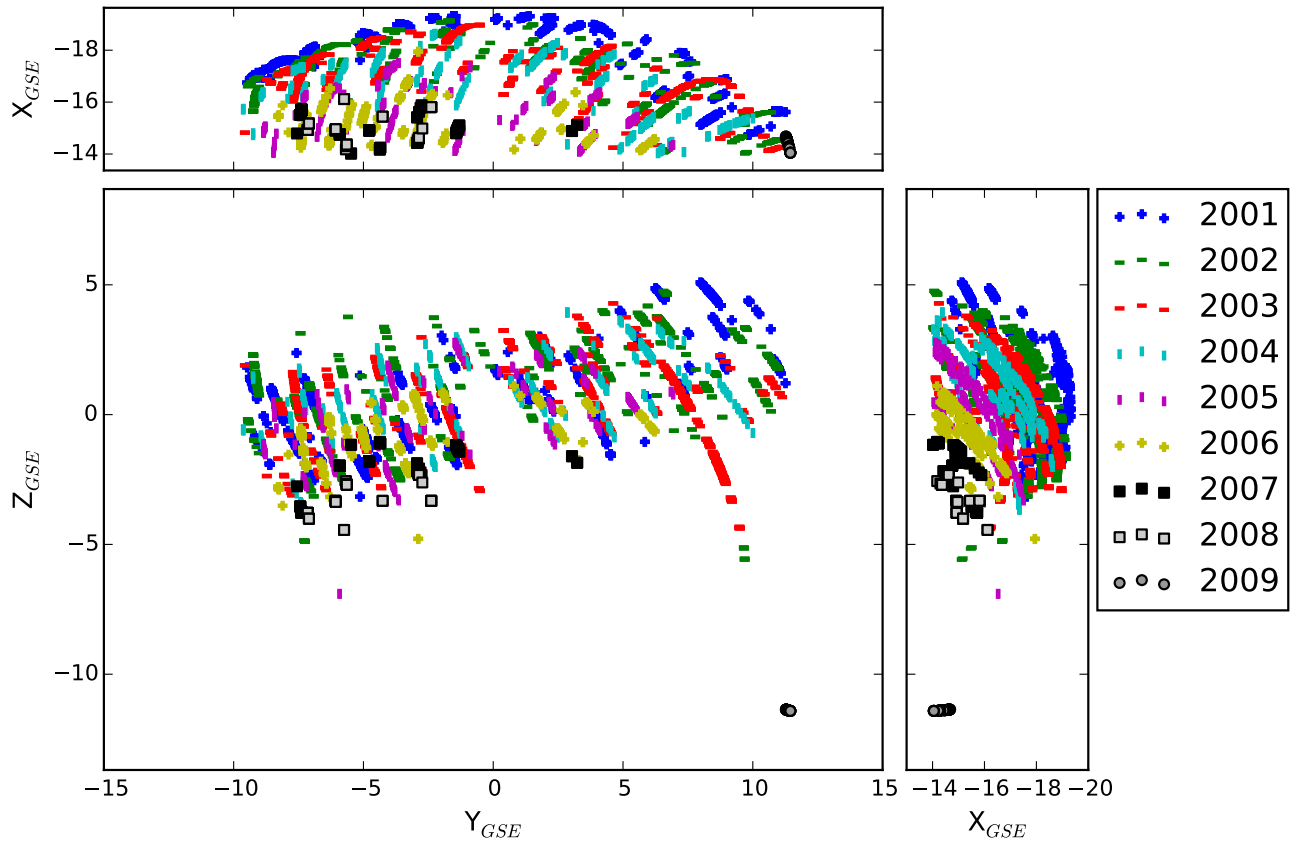


Figure 1. Locations of all 5030 neutral sheet crossings from 2001-2009, identified by sign reversals of the B_x component in the plasma sheet.

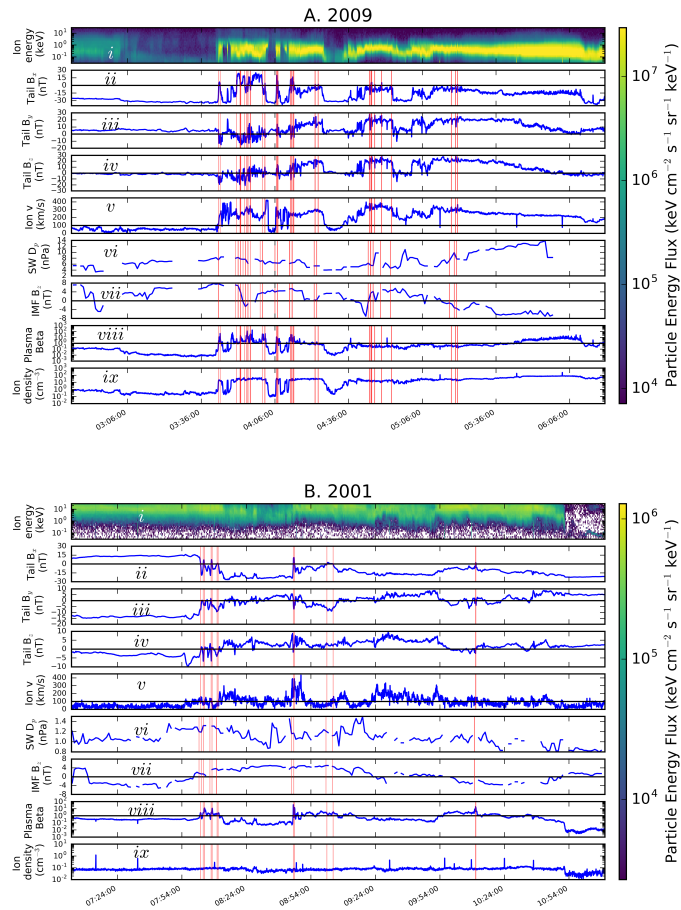


Figure 2. (A) Key parameters of all (48) candidate neutral sheet crossings observed by Cluster 3 from 2009 observed on 11/10/2009. (B) All the events from an exemplar orbit from 2001, which were observed on 13/10/2001.

For each year: panel (i) shows a spectrogram of the ion energies; panels (ii-iv) show the B_x , B_y and B_z components of the magnetic field in the plasma sheet; panel (v) shows the ion velocities; panel (vi) shows the solar wind dynamical pressure; panel (vii) shows the IMF B_z component; panel (viii) shows the plasma beta; and panel (ix) shows the plasma density. Note that the y-axis scales for most panels differ between years. Data shown are from Cluster 3, except for the solar wind dynamic pressure and IMF B_z component which are taken from the OMNI database.

The time of each event shown is indicated by a vertical red line. The spectrograms observed in

both years show that the events from 2009 have a much lower ion energy than in 2001. Coupled

D R A F T

October 20, 2016, 5:20pm

D R A F T

with the observation that the events in 2009 occurred much further away from the equatorial

plane than the other events (at $[-14, 11, -15]R_e$) this is indicative that these events are from the

magnetosheath which is outside of the magnetosphere.

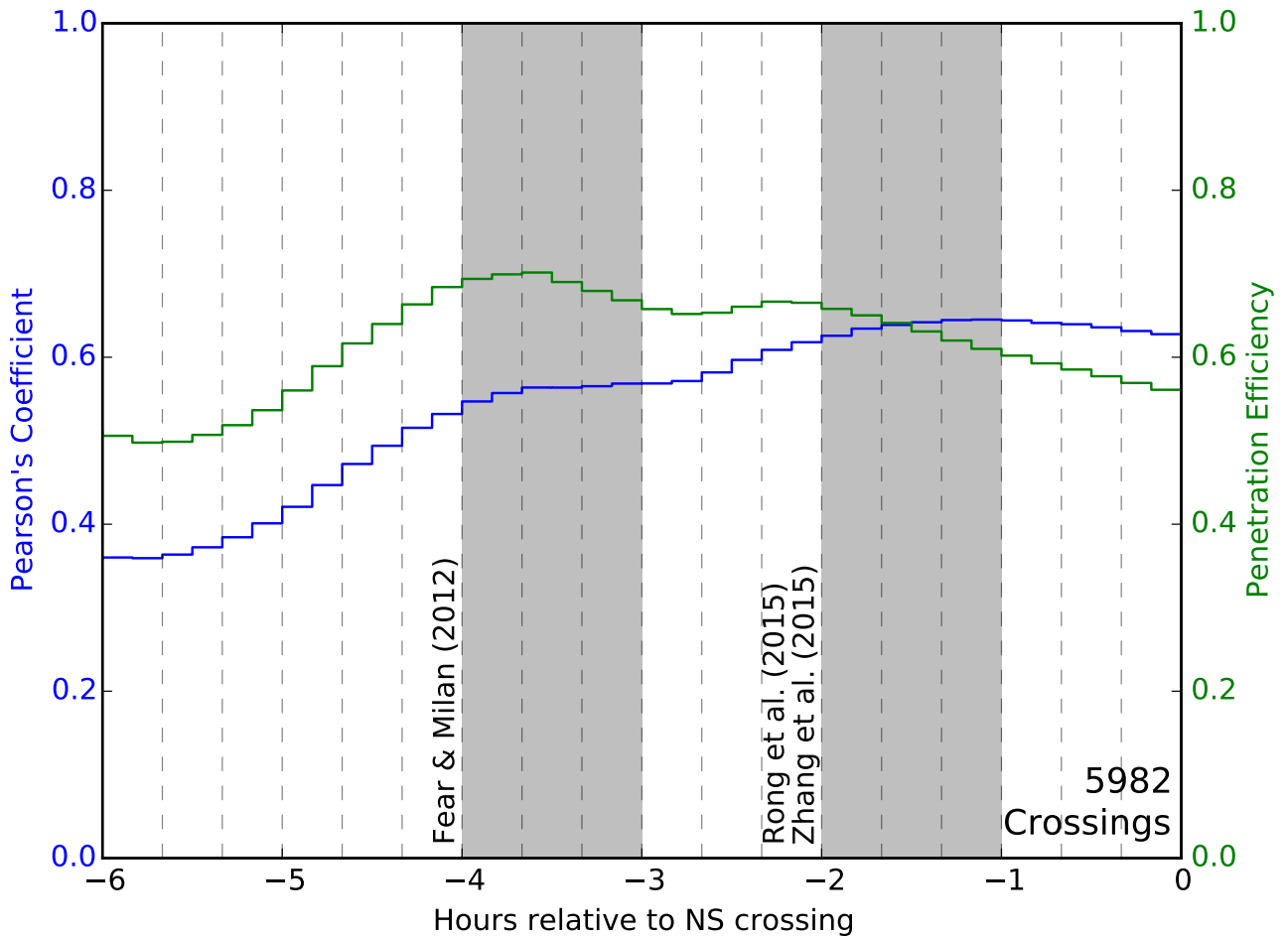


Figure 3. Correlation time series plot for all neutral sheet crossings. The blue series shows how the correlation coefficient varies as the IMF B_y data is lagged relative to the plasma sheet B_y data. The green series shows how the penetration efficiency changes as the lag applied to the IMF B_y data is varied. Peaks are seen at approximately 1-2 hours and 3-4 hours which are consistent with previous studies, indicated by grey shading.

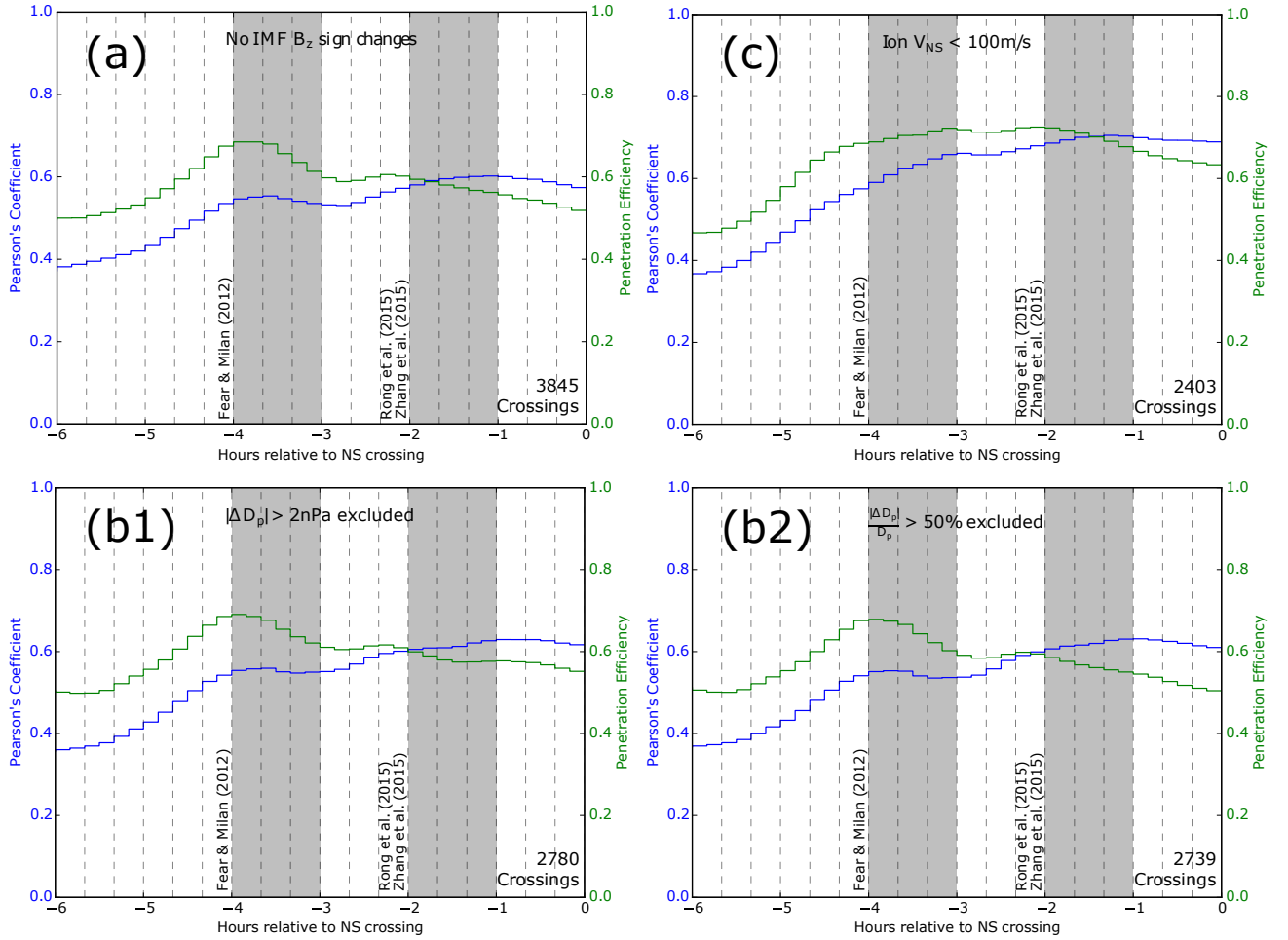


Figure 4. Each panel is in the same format as in Figure 3 but shows the effects of applying each of the filters chosen by *Cao et al.* [2014]. Panel (a) shows all events except those with an IMF B_z sign change in the 5 minutes before or after a neutral sheet crossing are excluded, panel (b1) shows all events except those where there was a change in the solar wind dynamical pressure of 2nPa within 5 minutes of a neutral sheet crossing, panel (b2) shows all events except where there was a relative solar wind pressure changes of more than 50% in the same 10 minute window and panel (c) shows all events except for those with fast ion flows ($>100\text{m s}^{-1}$) in the magnetotail at the time of the neutral sheet crossing have been excluded.

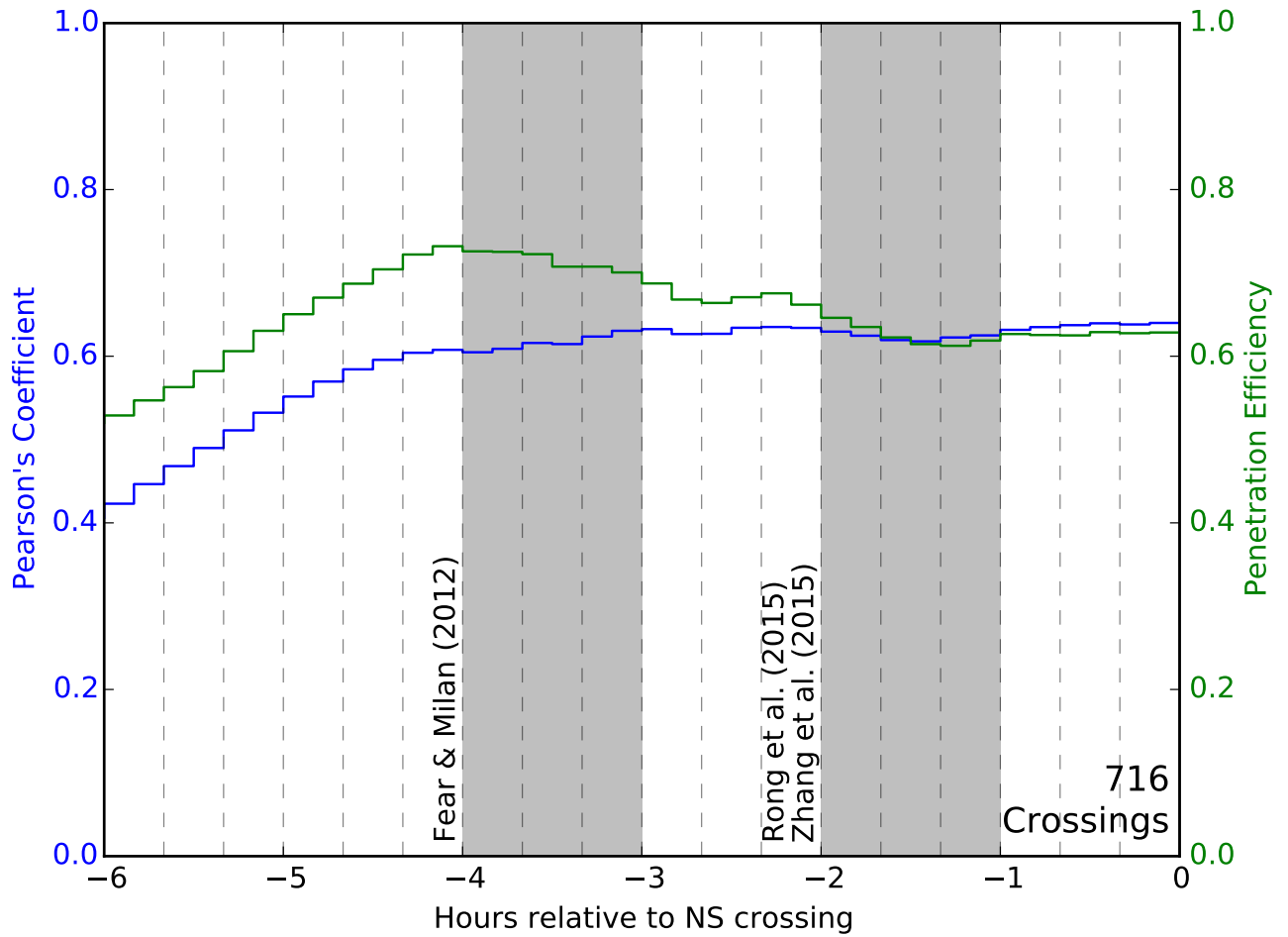


Figure 5. As in Figure 3, except all of the criteria defined by Cao et al. [2014] have been applied.

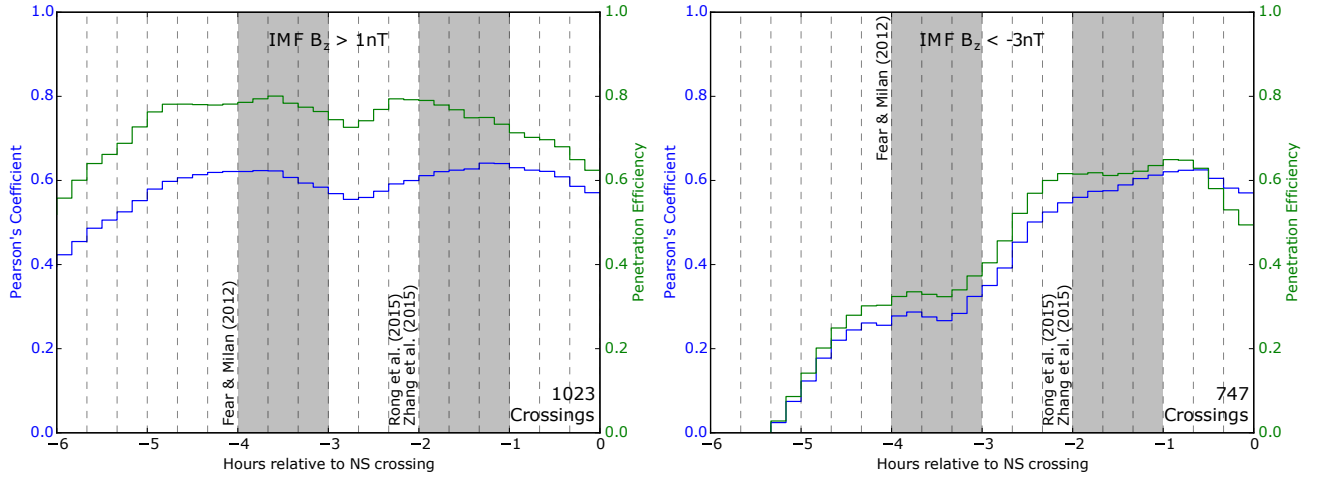


Figure 6. As in Figure 3, except with an IMF B_z criterion applied. The left plot shows the time series for events where IMF B_z was “generally northward”. A “generally northward” neutral sheet crossing was defined to be when 60% of the IMF B_z data had been greater than $1nT$ for two hours leading up to the crossing. The right hand plot shows the time series for events which occurred when the IMF was “generally southward”. Similarly, a “generally southward” neutral sheet crossing was defined to be when 60% of the IMF B_z data had been less than $-3nT$ for two hours leading up to the crossing. The correlation and penetration are elevated for a much longer time when IMF is northward compared to when the IMF is negative.

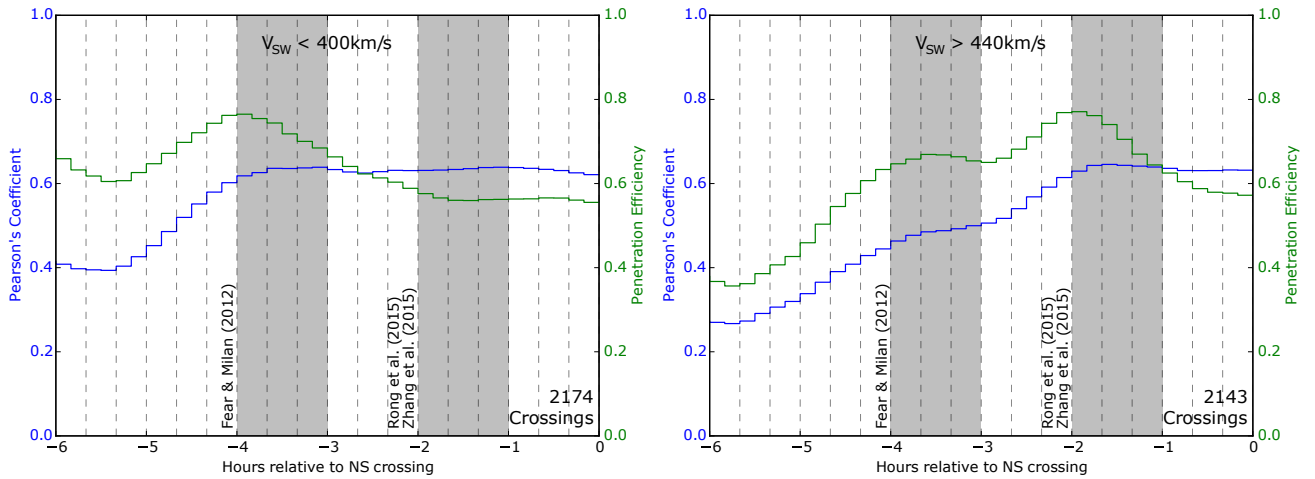


Figure 7. As in Figure 3, except with a solar wind velocity criteria applied. The left plot shows the time series for events where the solar wind was “generally fast” (a minimum of 60% of the data over two hours leading up to the neutral sheet crossing had to be $>440\text{km s}^{-1}$) and the right plot shows the time series for events when the solar wind was “generally slow” (a minimum of 60% of the data over two hours leading up to the neutral sheet crossing had to be $<400\text{km s}^{-1}$). The correlation and penetration are elevated for a much longer time when the solar wind is “generally slow” compared to when it is “generally fast”, when a much more prompt response is observed.

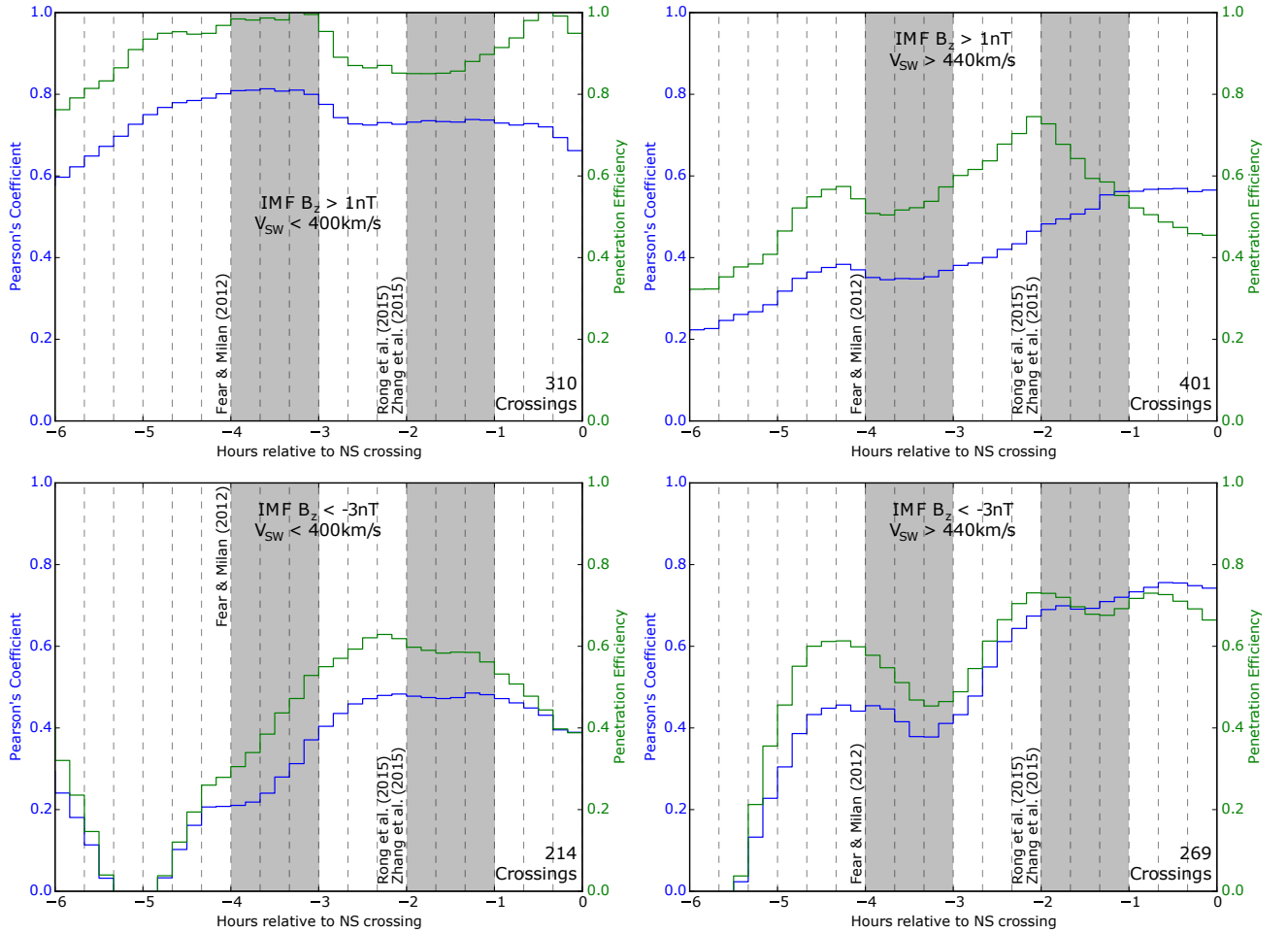


Figure 8. As in Figure 3, except the criteria in the previous two figures have been combined. The top left plot shows the correlation when dayside reconnection is unfavourable; a very long period of elevated correlation is observed. The lower right lag plot shows the correlation and penetration efficiency for events where dayside reconnection was highly favourable; a much more prompt correlation can be seen that decays quickly. The remaining two plots show events which satisfy the remaining combinations of each criteria; these show that the peaks in correlation lie between those found for events during times of favourable/unfavourable conditions for dayside reconnection to take place.

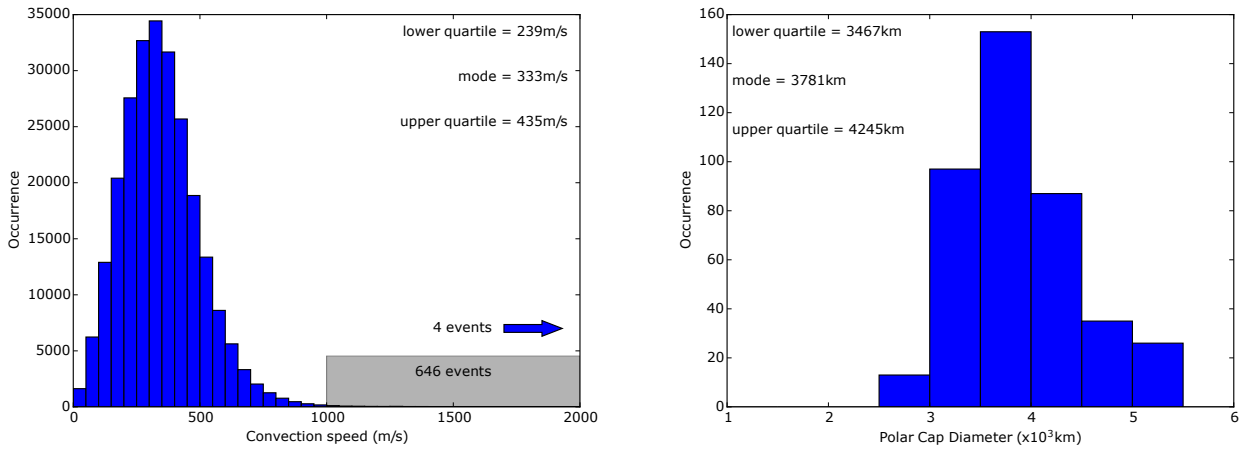


Figure 9. The left histogram shows occurrences of ionospheric convection speeds in the midnight sector at approximately 85 degrees of latitude, as measured by SuperDARN from 1999 to 2006. The right histogram showing the occurrences of the diameter of the polar cap over a total of 73 hours of observations taken between 1998 and 2002 during a variety of geophysical conditions; these data are reproduced from Figure 3 of *Milan et al.* [2007], but the x-axis values of magnetic flux content have been converted to polar cap diameter.

Table 1. Estimates for the field line convection time over the polar cap.

		Field line convection speed		
		240m/s	330m/s	440m/s
$Area_{pc}$	$9.4 \times 10^{12} m^2$	4hrs	2hrs 50mins	2hrs 10mins
	$1.1 \times 10^{13} m^2$	4hrs 20mins	3hrs 10mins	2hrs 20mins
	$1.4 \times 10^{13} m^2$	5hrs	3hrs 30mins	2hrs 40mins